EMBO reports

scientific report

A model for the topology of active ribosomal RNA genes

Serguei Denissov[1], Frédéric Lessard[2], Christine Mayer[3], Victor Stefanovsky[2], Marc van Driel[1†], Ingrid Grummt[3], Tom Moss[2] & Hendrik G. Stunnenberg[1+]

[1]Science Faculty, Department of Molecular Biology, Nijmegen Centre for Molecular Life Sciences, Radboud University, Nijmegen, The Netherlands, [2]Cancer Research Centre and Department of Molecular Biology of Laval University, Québec, Canada, and [3]Division of Molecular Biology of the Cell II, DKFZ-ZMBH Alliance, German Cancer Research Center, Heidelberg, Germany

The Christmas tree view of active ribosomal RNA (rRNA) genes suggests a gene topology in which a large number of nascent rRNA transcripts are prevented from intertwining. The way in which this is achieved has remained unclear. By using a combination of chromatin immunoprecipitation and chromosome conformation capture techniques, we show that the promoter, upstream region and terminator R3 of active rRNA genes are held together spatially throughout the cell cycle, forming a stable core around which the transcribed region is organized. We suggest a new core–helix model for the topology of rRNA genes, that provides a structural basis for the productive synthesis or rRNA.

Keywords: rRNA genes; Christmas trees; RNA polymerase I; core–helix model; rDNA topology

EMBO *reports* (2011) **12**, 231–237. doi:10.1038/embor.2011.8

INTRODUCTION

Ribosome biogenesis is a highly coordinated, multistep process that takes place in the nucleolus, where ribosomal RNAs (rRNAs) are synthesized, processed and assembled into ribosomal subunits. rRNA genes are clustered at acrocentric chromosomes, forming the nucleolus organizer regions, in which the nucleoli are assembled (Raška, 2003). In electron microscopy, nucleoli have three compartments that are visible as distinct areas. The central electron microscopy-transparent area, called the fibrillar centre, contains ribosomal DNA (rDNA) fibrils, but low levels of protein and RNA (Derenzini *et al*, 2006). Active transcription occurs at the boundary between the fibrillar centre and the adjacent dense fibrillar components (DFCs), an electron-dense area surrounding the fibrillar centre that consists of ribonucleoprotein (RNP) complexes—the processing factories of the pre-rRNA. The DFC is surrounded by the granular components comprising pre-ribosomal particles at different stages of maturation (Olson, 2004).

Initiation of rDNA transcription requires the assembly of the preinitiation complex at the rDNA promoter via the synergistic action of the upstream binding factor (UBF) and the promoter selectivity factor SL1. UBF binds to the rDNA promoter, the enhancer region and throughout the transcribed region to maintain rDNA gene activity and architecture (Mais *et al*, 2005; Russell & Zomerdijk, 2005; Moss *et al*, 2007). Promoter specificity is conferred by SL1, a protein complex containing the TATA binding protein (TBP) and five TBP-associated factors (TAF_Is). Regulation of rRNA synthesis in response to external signals is brought about by the transcription initiation factor Rrn3/TIF-IA, which interacts with both RNA polymerase I (RNAP I) and two TAF_Is, thereby bridging RNAP I to the preinitiation complex at the rDNA promoter (Moss *et al*, 2007). To complete transcription, the termination factor TTF-I binds to specific terminator elements, called Sal-boxes, to stop elongation and mediate release of RNAP I and rRNA. In humans and mouse, the Sal-boxes are grouped into three tandem terminator regions R1, R2 and R3; RNAP I terminates predominantly at R1.

In this study, we present chromatin immunoprecipitation (ChIP), chromosome conformation capture (3C) and cell-imaging data that provide insight into the structure–function relationship of the active rDNA loci. On the basis of our data and previous knowledge, we propose a new model describing the higher-order structural organization of active rDNA genes.

RESULTS AND DISCUSSION

Binding profiles of the RNAP I transcription factors

Previously, we have used ChIP followed by cloning and sequencing of the precipitated genomic fragments to identify the binding sites for TBP in the human genome (Denissov *et al*, 2007). We found that approximately 10% of all clones mapped to the

[1]Science Faculty, Department of Molecular Biology, Nijmegen Centre for Molecular Life Sciences, Radboud University (274), PO Box 9101, Nijmegen 6500 HB, The Netherlands
[2]Cancer Research Centre and Department of Molecular Biology of Laval University, 9 rue McMahon, 1744 Québec, PQ, Canada
[3]Division of Molecular Biology of the Cell II, DKFZ-ZMBH Alliance, German Cancer Research Center, Im Neuenheimer Feld 280, D-69120 Heidelberg, Germany
[†]Present address: Netherlands Bioinformatics Centre, PO Box 9101, 6500 HR, Nijmegen, The Netherlands
[+]Corresponding author. Tel: +31 243 610 524; Fax: +31 243 610 520; E-mail: h.stunnenberg@ncmls.ru.nl

Received 7 August 2010; revised 10 January 2011; accepted 13 January 2011; published online 18 February 2011

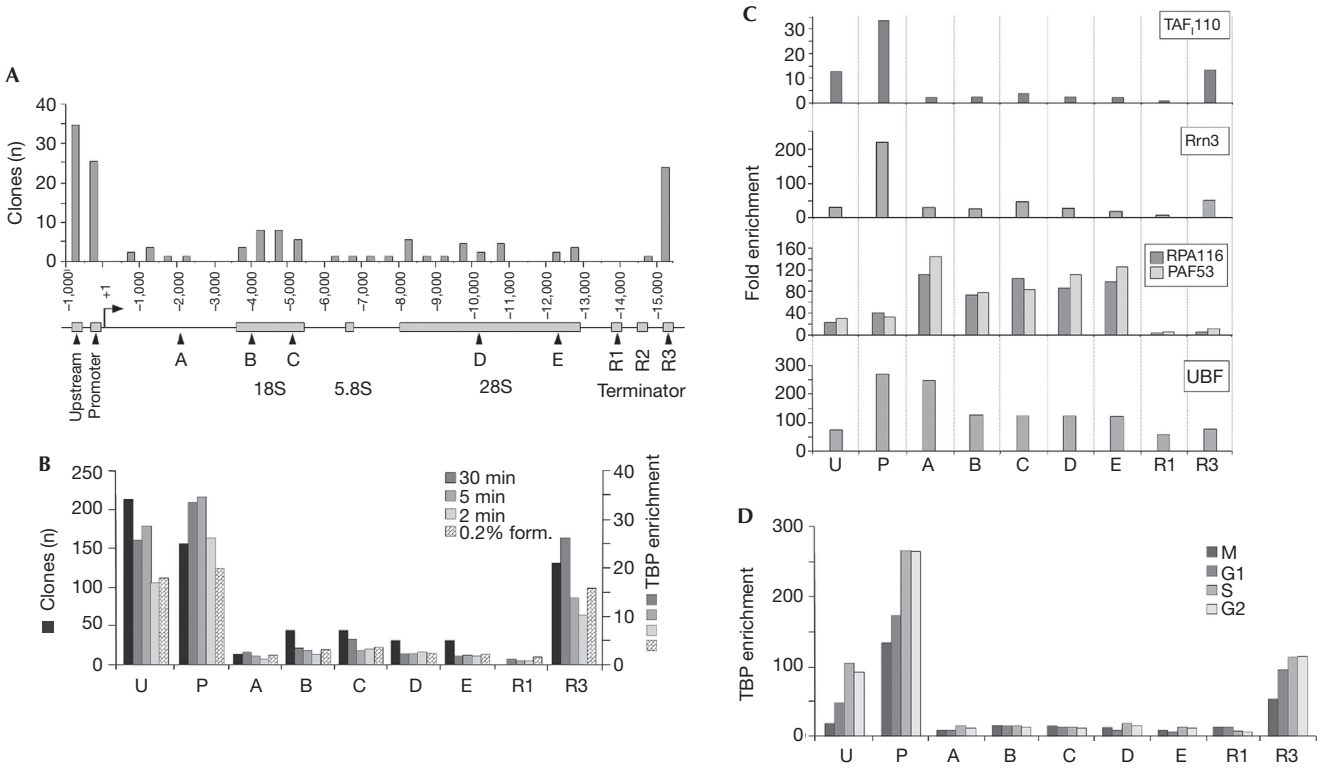

Fig 1 | Binding of RNA polymerase I transcription factors to ribosomal DNA. (**A**) DNA fragments precipitated by TBP-ChIP were cloned (Denissov *et al*, 2007), sequenced and aligned to the rRNA unit. The number of reads is counted per 500 bp. Organization of rDNA: the upstream region (U), the promoter (P), the terminators R1–R3 and the rDNA coding regions are shown by grey boxes. Arrowheads point to genomic locations (**A–E**) that were validated by ChIP-qPCR analysis. The arrow indicates the transcription start site at +1 position. (**B**) Enrichment of TBP by ChIP-qPCR (grey bars, right scale) was plotted against the numbers of cloned DNA fragments (black bars, left scale) at the positions shown in (**A**). (**C**) Graph showing the enrichment of RNAP I factors as in (**B**). (**D**) Binding of TBP to rDNA in different phases of the cell cycle. ChIP, chromatin immunoprecipitation; qPCR, quantitative PCR; rDNA, ribosomal DNA; RNAP I, RNA polymerase I; rRNA, ribosomal RNA; TAF$_I$, TBP-associated factor; TBP, TATA binding protein; UBF, upstream binding factor.

rRNA gene. Alignment to the rDNA unit revealed that most of the clones (approximately 60%) were distributed over three regulatory elements: the rDNA promoter, upstream region and terminator R3 (Fig 1A). The remaining clones aligned to the transcribed region, but not to the intergenic spacer that separates individual transcription units. TBP enrichment was validated by ChIP and quantitative PCR (qPCR) analyses at all probed positions, the highest values were found at the promoter, upstream region and terminator R3, and low levels were found throughout the coding region (Fig 1B). Remarkably, no enrichment was found at terminator R1, suggesting a specific targeting mechanism towards R3. To rule out the possibility that TBP binding was caused artificially by extensive crosslinking, we then used short treatments or a low concentration of formaldehyde. As expected, the overall recoveries decreased (supplementary Fig S1 online); however, the specific enrichment remained high and showed the same pattern (Fig 1B). In support of this observation, the TAF$_I$110 subunit of SL1 complex showed a similar binding profile to TBP (Fig 1C); *TAF$_I$110* has previously been reported to bind to the upstream enhancer/spacer promoter (Mais *et al*, 2005).

Next, we measured the binding of other RNAP I transcription factors (Fig 1C). Rrn3/TIF-IA associated mainly with the promoter, in line with its reported interactions with SL1 and initiation-competent RNAP I (Moss *et al*, 2007). The RNAP I subunits RPA116 and PAF53 showed a high enrichment throughout the transcribed region, in accordance with the high density of elongating polymerases on the rRNA gene as well as at the promoter and the upstream region (Mais *et al*, 2005). RNAP I binding was low at the terminator regions R1–R3 suggesting that it dissociates at or around R1. High enrichment of UBF was detected at the promoter region, as well as throughout the rRNA locus, in line with the role of UBF in transcription and nucleolus organizer region architecture (Mais *et al*, 2005).

Binding of TBP to rDNA during cell cycle progression

A remarkable feature of the rRNA genes is that they are not compacted during chromosome condensation in metaphase (Derenzini *et al*, 2006) and that transcription factors remain associated with rDNA during mitosis, while rRNA synthesis is blocked (Roussel *et al*, 1996). To investigate the binding characteristics of TBP during the cell cycle, we performed ChIP analysis on synchronized cells (supplementary Fig S2 online). In metaphase, a high enrichment of TBP was detected at both the promoter and terminator, whereas binding to the upstream region was not apparent (Fig 1D). During G1, S and G2 phases, the binding of TBP increased at the promoter and terminator by

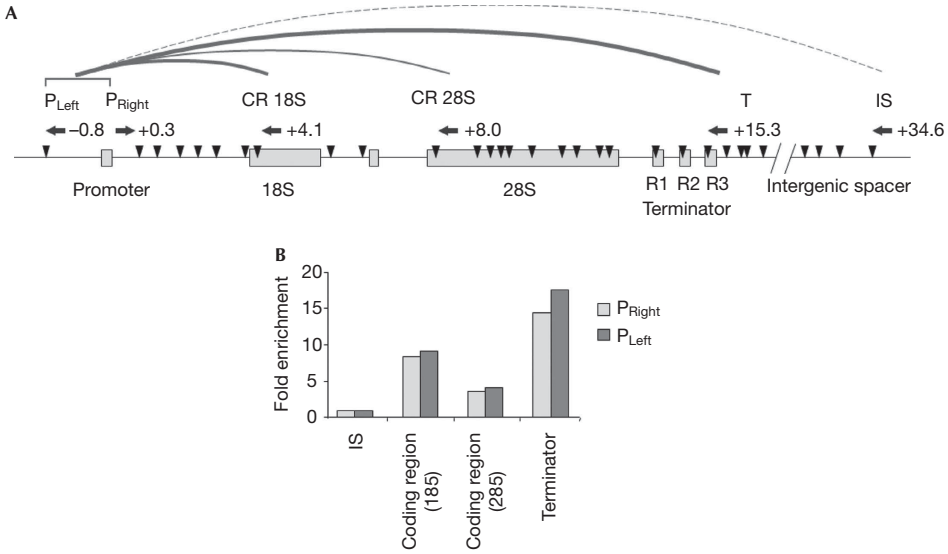

Fig 2 | Spatial proximity of the ribosomal DNA regions. (**A**) Schematic presentation of the 3C assay. The thickness of the arcs linking the promoter to other regions of rDNA represents the ligation efficiency. Arrows indicate the primers used to amplify two regions flanking the promoter (P_{Left} and P_{Right}), the coding region, the terminator R3 (T) and a region in the intergenic spacer (IS). The location of the primers (in kb) is indicated next to the arrows. The organization of rRNA gene is shown with grey boxes and named below. Arrowheads point to the HpyCH4IV restriction sites. (**B**) Ligation frequencies between promoter (P_{Left} and P_{Right}) and other rDNA regions are plotted as fold over background (intergenic spacer). 3C, chromosome conformation capture; CR, coding region, IS, intergenic spacer; rDNA, ribosomal DNA; rRNA, ribosomal RNA.

approximately twofold. Remarkably, enhanced TBP-binding was more pronounced at the upstream region, and increased approximately sixfold to maximal levels in S and G2 phases. Enrichment at the transcribed region remained mostly unchanged during the cell cycle. Although variable accessibility of epitopes cannot be ruled out, these data suggest a stable association of the SL1 complex with the rDNA promoter, terminator and upstream region during the active rRNA transcription and suggest that the association of SL1 to the upstream region is transcription-dependent and contributes to regulation of rDNA transcription during the cell cycle.

Distant rDNA regions are in close spatial proximity

The efficient crosslinking of TBP and TAF_I110 to the different regions of the rRNA gene indicates that these regions are in close proximity, as suggested previously (Németh *et al*, 2008). To gain insight into the structural organization of active rDNA repeats, we performed the 3C assays at high resolution using HpyCH4IV endonuclease which evenly digests the gene into 21 fragments (Fig 2A). Quantification of the ligation frequencies between different rDNA sites for both ends of the promoter fragment revealed a 15–18-fold enrichment for interactions between the promoter and terminator, and a 5–10-fold enrichment between promoter and transcribed region (Fig 2B), in line with the ChIP-cloning frequencies and the binding profiles of SL1 (Fig 1). These results were confirmed by the 3C with *Bam*HI endonuclease (supplementary Fig S3 online). Together, our ChIP and 3C data corroborate and extend previous observations proposing simultaneous interactions of SL1 complex with the promoter and terminator. In addition, the high-resolution 3C assay allowed us to observe spatial interactions between the promoter and the transcribed region suggesting a spatially compact conformation of the active rRNA genes. We named the putative SL1–promoter–terminator–upstream region structure the 'anchoring core'.

We cannot formally exclude the possibility that the observed promoter–terminator interactions occur between the elements of different rDNA repeats. However, we consider this to be unlikely because electron microscopy tomography data suggest that discrete fibrillar centre and DFC nucleolar compartments are formed around single rRNA genes (Cheutin *et al*, 2002).

Nucleolar stress alters the topology of rRNA genes

To investigate the effect of ongoing transcription on the intragenic molecular interactions, we suppressed rDNA transcription by treating cells with different transcription inhibitors. All inhibitors reduced the steady-state level of pre-rRNA by 40–90% (supplementary Fig S4A online). A concomitant reduction of RNAP I binding within the coding region was observed, whereas binding to the promoter and upstream region was not affected (Fig 3A). Surprisingly, binding of SL1—monitored by ChIP of TBP and TAF_I110—to the transcribed region was enhanced fivefold after treatment with both H_2O_2 and actinomycin D, whereas the association with the promoter, the upstream region and the terminator was not altered (Fig 3B). Increased binding to the transcribed region after H_2O_2 treatment was also observed for Rrn3/TIF-IA (supplementary Fig S4B,C online), whereas UBF binding was not affected by any of the inhibitors (Fig 3C). By contrast, rapamycin and anisomycin treatments did not increase binding of SL1 to the transcribed region. This result emphasizes that transcriptional inhibition in response to genotoxic and nutritional stress is brought about by different molecular mechanisms. Rapamycin impairs transcription initiation by preventing

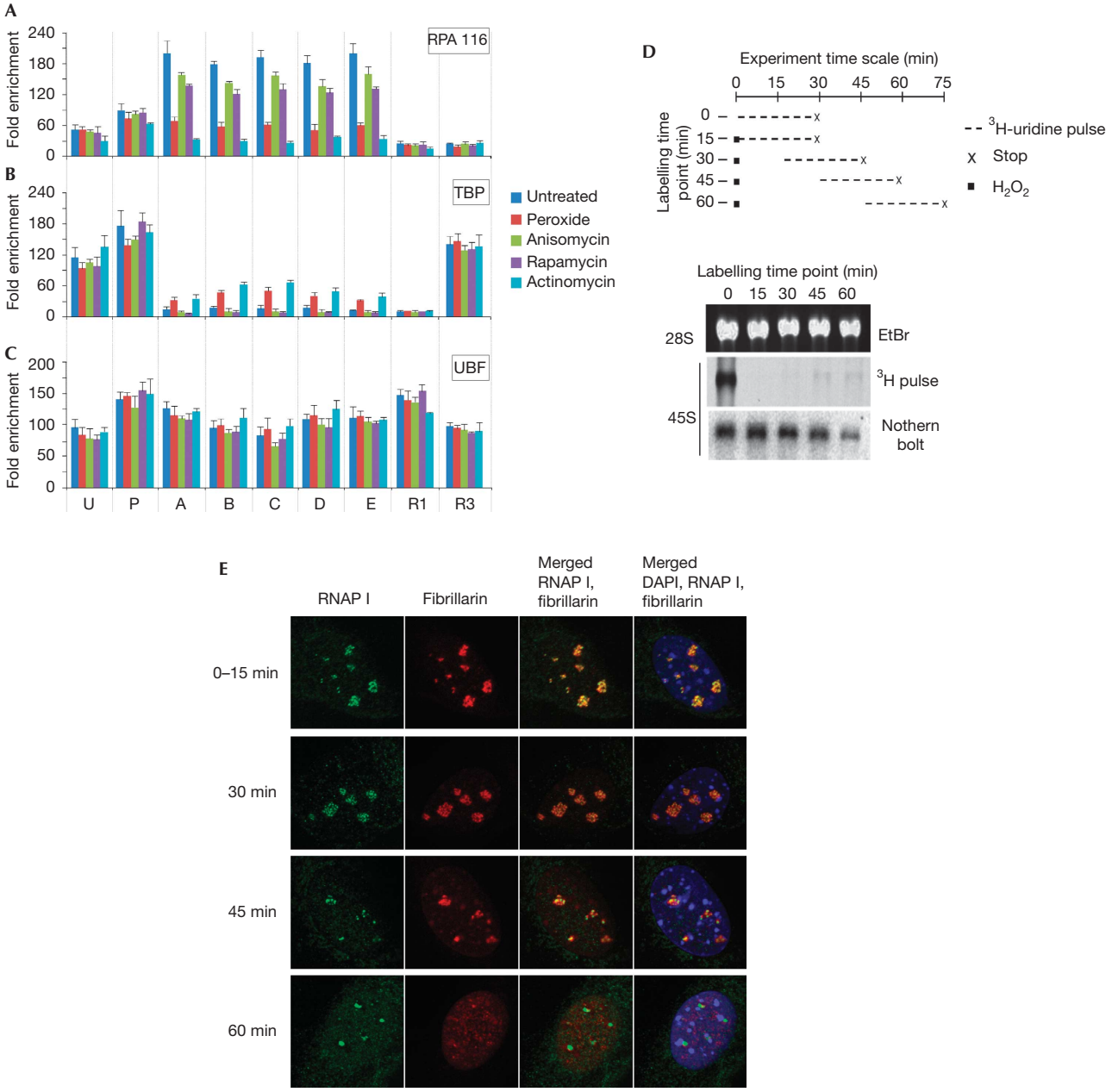

Fig 3 | Genotoxic stress leads to enhanced association of SL1 with the coding region. (**A–C**) Binding of RNAP I (RPA116), SL1 (TBP) and UBF to rDNA in untreated cells and cells treated with different transcription inhibitors. The error bars represent a standard deviation of ChIP-enrichment values. (**D**) Metabolic labelling of pre-rRNA after treatment with H_2O_2. (**E**) Immunofluorescent imaging of RNAP I (green) and fibrillarin (red) at different times after H_2O_2 treatment. ChIP, chromatin immunoprecipitation; DAPI, 4′-6-diamidino-2-phenylindole; EtBr, ethidium bromide; rDNA, ribosomal DNA; rRNA, ribosomal RNA; RNAP I, RNA polymerase I; TBP, TATA binding protein; UBF, upstream binding factor.

mTOR-dependent phosphorylation of Rrn3/TIF-IA (Mayer *et al*, 2004), whereas genotoxic stress leads to inactivation of TIF-IA/Rrn3 by JNK2-mediated phosphorylation (Mayer *et al*, 2005). We found that H_2O_2 treatment did not affect the promoter occupancy of SL1 and RNAP I, in contrast to previous studies in HEK293T cells. This might be due to the fact that U2OS cells express low levels of JNK2 (Wang *et al*, 2008; our unpublished data). Therefore, transcription inhibition should occur at the level of elongation. In support of this view, H_2O_2 treatment had the same effect on TBP binding as actinomycin D, a drug that is known to inhibit transcription elongation leading to the accumulation of abortive transcripts (Hadjiolova *et al*, 1995). Actinomycin D and other DNA intercalators trigger the release of elongating polymerases from rDNA and perturb nucleolar structure, leading to segregation, condensation and collapse of nucleolar compartments (Bernard & Granboulan, 1968; Jensen *et al*, 1985).

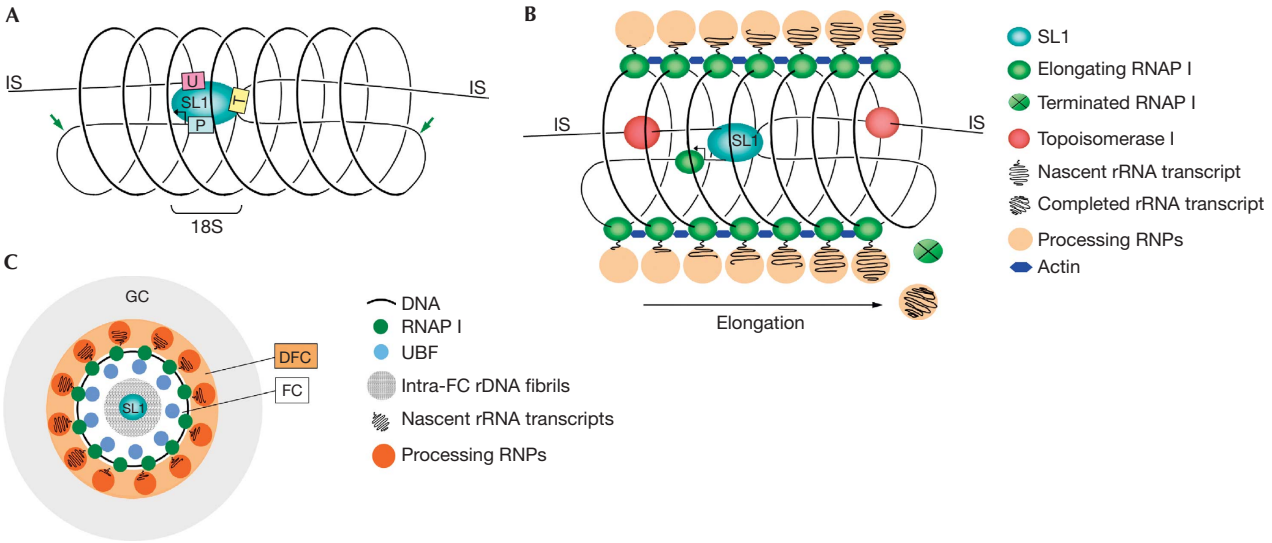

Fig 4 | The core–helix model describing the topology of active ribosomal RNA genes. (**A**) The core–helix rDNA structure. The anchoring core is formed by SL1 bound to the promoter (P), the upstream region (U) and the terminator R3 (T). Non-intersecting DNA rings comprising the transcribed region are cylindrically wrapped around the core; the 18S genomic region locates close to SL1. DNA fibrils (green arrows) enter into the core of the helix from its lateral sides. (**B**) Core–helix organization of transcribed rRNA genes. RNA polymerases initiate at the promoter in the core and elongate along the cylindrical helix (long arrow). Zig-zag black lines represent growing rRNA chains attached to RNA polymerases that are cotranscriptionally assembled into processing ribonucleoprotein particles. After termination, RNA polymerases dissociate from rDNA. Topoisomerase I removes torsional stress in the intergenic spacer resulting from the rotation of the rDNA solenoid. In addition, Topoisomerase I is required throughout the transcribed region (not indicated). (**C**) Scheme of the nucleolar compartments in frontal projection of the core–helix structure. The central area corresponds to the FCs with SL1 and DNA fibrils of the anchoring core. The transcribed region and elongating RNA polymerases are at the periphery of the FC. Nascent rRNA chains of increasing length are assembled into processing RNPs that form the DFC compartment. DFC, dense fibrillar centre; FC, fibrillar centre; GC, granular component; IS, intergenic spacer; rDNA, ribosomal DNA; RNAP, RNA polymerase; RNP, ribonucleoprotein complex; rRNA, ribosomal RNA; UBF, upstream binding factor.

To examine the link between H_2O_2 treatment and nucleolar structure, we performed pulse-labelling experiments, monitoring the synthesis of 45S pre-rRNA at different times after H_2O_2 treatment. Transcription was blocked immediately on H_2O_2 treatment and pre-rRNA levels decreased with normal half-life (Fig 3D and data not shown). After H_2O_2 treatment, the typical sub-nucleolar RNAP I dots condensed into intensely stained small dots (Fig 3E; supplementary Fig S5 online). Delocalization of fibrillarin lagged behind sub-nucleolar condensation, consistent with pre-formed pre-rRNA retaining fibrillarin in the DFC regardless of transcriptional activity (Olson, 2004). These data indicate that after H_2O_2 and actinomycin D treatment the nucleolar substructure collapsed on to the anchoring core leading to increased crosslinking of SL1 to the transcribed region.

The core–helix model

The spatial organization of active rRNA genes has been the focus of intense investigation. It has remained unclear, however, how the pre-rRNAs synthesized by about 100 elongating polymerases can be kept disentangled in the limited nucleolar space. It is remarkable how effectively the active rRNA genes can be spread to reveal two-dimensional 'Christmas tree' views in which the nascent rRNA molecules are spatially separated (Raška, 2003). On the basis of our data and previous publications, we propose a novel structural organization of the active rRNA genes—the core–helix model.

In this model, the key initiation complex SL1 binds to the promoter, terminator R3 and upstream region and functions as the anchoring core of the rDNA structure (Fig 4A). In accord with electron microscopy-tomographic data showing that active rRNA genes have a cylindrical structure (Cheutin *et al*, 2002), we propose that the transcribed rDNA region is wrapped around the anchoring SL1-based core, lining up into consecutive rows of non-intersecting rings in a 'helix'-like cylindrical manner (Fig 4A). This helical structure places the transcribed region in spatial proximity to the SL1/anchoring core. The open lateral sides of the cylinder would facilitate the access of transcription factors to the internally located promoter in order to assemble the initiation complex. In this model, RNAPs initiate at the promoter located in the core of the rDNA cylindrical helix, move to the outer rim of the helix, then track laterally and drop off at the other end of the helix, near to terminator R1 (Fig 4B). This provides a simple and efficient way of accommodating the large number of elongating RNAPs allowing the nascent transcripts to radiate away from the helix into the processing area. The numerous large processing RNPs that attach co-transcriptionally to the pre-rRNAs are unlikely to be dragged along the helix through the dense nucleolar environment, but are proposed to remain localized spatially at the same face of the helix. The pulling forces of the RNAPs would then rotate the entire core–helix structure around its axis, with the torsional stress in the transcribed region and intergenic spacers being relaxed by nucleolar topoisomerase I, directed at both negative and positive

supercoils (Zhang *et al*, 1998). Elongating polymerases can be organized on the rDNA helix—possibly by nucleolar actin that is required for RNAP I elongation (Ye *et al*, 2008), as seen in electron microscopy data—on which the RNAP I molecules are lined up into rows on the surface of the cylindrical rDNA (Cheutin *et al*, 2002).

The proposed core–helix structure provides a plausible explanation of the increased SL1 binding over the rRNA-transcribed region that is, counter-intuitively, increased, whereas transcription is decreased. We suggest that peroxide and actinomycin D might have destabilized the protein framework that holds the rDNA helix in place, displaced the elongating RNAPs from DNA and consequently caused a collapse of the rDNA onto the SL1 core. In agreement with this, the active RNAP I molecules are required to prevent nucleolar collapse (Olson, 2004) and, therefore, possibly also to maintain the rDNA 'helix' structure.

The core–helix model integrates well into nucleolar morphology. As discrete DFCs are formed around single rRNA genes (Cheutin *et al*, 2002), the central area comprising the anchoring core might correspond to the electron microscopy-transparent fibrillar centre compartment (Fig 4C) in which SL1 and other transcription factors, as well as transcription-initiation events, were mapped (Derenzini *et al*, 2006). SL1 remains in the fibrillar centre in metaphase (Roussel *et al*, 1996) and also remains bound to the promoter and terminator (Fig 1C), suggesting that the rDNA fibrils observed in the centre of the fibrillar centre (Heliot *et al*, 1997; Olson, 2004) could be the promoter, upstream region and terminator. Nascent transcripts radiating away from the rDNA helix can co-transcriptionally form the processing RNPs that together comprise the DFC compartment around each fibrillar centre (Fig 4B,C). In support of this view, nascent pre-rRNA transcripts and processing RNPs were invariably mapped to DFC, whereas the rDNA transcribed region with elongating polymerases and the process of rRNA synthesis have all been mapped to the periphery of the fibrillar centre in a narrow border between the fibrillar centre and DFC (Raška, 2003). In this manner, the transcripts would not be entangled and could be spread easily to form the two-dimensional 'Christmas trees' seen in the electron microscopy images on disruption of the core structure and stretching out of the rDNA gene helix.

In conclusion, we propose a three-dimensional core–helix structure of the actively transcribed rRNA genes in which promoter, upstream region and terminator are linked together by SL1 and surrounded by a rotating cylindrically shaped rDNA-transcribed region. This structure reinforces the results of numerous studies of nucleolar morphology and functions, resolving the structural basis for efficient rRNA synthesis.

METHODS

Antibodies and inhibitors. TAF_I110, Rrn3, UBF, RPA116, PAF53 and RPA194 antibodies were generated in the labs of I. Grummt and T. Moss. TBP (SL30) and fibrillarin (MMS-581S) antibodies were obtained from Diagenode and Covance. Cells were treated for 1.5 h under the following conditions: 0.2 mM peroxide, 40 ng/ml actinomycin D, 40 nM rapamycin and 10 μM anisomycin.

ChIP and qPCR. ChIP experiments were performed as described (Denissov *et al*, 2007). The peroxide treatments were repeated four times (biological replicas). The other inhibitors were repeated twice. Primer sequences used in qPCR for ChIP and pre-rRNA expression are listed in supplementary Table 1 online.

Cell-cycle synchronization. U2OS cells at 80% confluence were arrested in metaphase by 40 ng/ml nocodazole for 18 h in DMEM + 10% FCS. The round-shaped cells were collected and either directly crosslinked (M phase) or cultured in nocodazole-free medium for 8 h (G1 phase) before crosslinking. Synchronization in G2 and S phases was achieved by a double thymidine block (2.5 mM thymidine treatment for 18 h with 12-h interval) and release for 4 and 7.5 h, respectively.

3C assay. 3C analysis was carried out according to standard protocols, with minor modifications. Digested chromatin from 10^7 cells was diluted and ligated for 2 h at 16 °C. The crosslinks were reversed for 4 h at 65 °C, DNA was phenol-extracted, ethanol-precipitated and 1/40 of the sample was used for qPCR. For each site, three primers were designed and tested in different combinations for the optimal efficiencies (supplementary Table 2 online).

Immunofluorescence. NIH3T3 cells grown on coverslips were fixed with 4% paraformaldehyde for 15 min and permeabilized with 0.5% Triton for 5 min. Cells were blocked in 5% goat serum/PBS, incubated with RPA116 and fibrillarin antibodies (1:100, 1 h), stained with secondary antibodies (Alexa Fluor 488 and 568) and examined by using an Olympus FV1000 microscope.

Metabolic labelling of RNA. Cells were labelled for 30 min with 2.5 μCi/ml ^{3}H-uridine and rRNA was analysed as described (Gagnon-Kugler *et al*, 2009).

Northern blotting. In all, 2–4 mg of total RNA was run on 1% formaldehyde–MOPS gel, transferred to a Biodyne membrane and hybridized at 65 °C with random-prime-labelled DNA in 250 mM $NaHPO_4$ (pH 7.2), 7% SDS and 10 mM EDTA using the probe +469–1239 relative to the transcription start site. Membranes were analysed by phospho-imaging. RNA amounts were normalized to EtBr-stained 18S rRNA.

Supplementary information is available at EMBO *reports* online (http://www.emboreports.org).

ACKNOWLEDGEMENTS

This work was supported by (NGI 050-71-016) and European Union FP6-IP HEROIC (LSHG-CT-2005-018883) grants.

CONFLICT OF INTEREST

The authors declare that they have no conflict of interest.

REFERENCES

Bernard W, Granboulan N (1968) Electron microscopy of the nucleolus in vertebrate cells. In *Ultrastructure in Biological Systems*, Dalton A, Haguenav F (eds) Vol 3, pp 81–149. New York and London: Academic Press

Cheutin T, O'Donohue MF, Beorchia A, Vandelaer M, Kaplan H, Defever B, Ploton D, Thiry M (2002) Three-dimensional organization of active rRNA genes within the nucleolus. *J Cell Sci* **115:** 3297–3307

Denissov S, van Driel M, Voit R, Hekkelman M, Hulsen T, Hernandez N, Grummt I, Wehrens R, Stunnenberg H (2007) Identification of novel functional TBP-binding sites and general factor repertoires. *EMBO J* **26:** 944–954

Derenzini M, Pasquinelli G, O'Donohue MF, Ploton D, Thiry M (2006) Structural and functional organization of ribosomal genes within the mammalian cell nucleolus. *J Histochem Cytochem* **54:** 131–145

Gagnon-Kugler T, Langlois F, Stefanovsky V, Lessard F, Moss T (2009) Loss of human ribosomal gene CpG methylation enhances cryptic RNA polymerase II transcription and disrupts ribosomal RNA processing. *Mol Cell* **35:** 414–425

Hadjiolova KV, Hadjiolov AA, Bachellerie JP (1995) Actinomycin D stimulates the transcription of rRNA minigenes transfected into mouse

cells. Implications for the *in vivo* hypersensitivity of rRNA gene transcription. *Eur J Biochem* **228:** 605–615

Heliot L, Kaplan H, Lucas L, Klein C, Beorchia A, Doco-Fenzy M, Menager M, Thiry M, O'Donohue MF, Ploton D (1997) Electron tomography of metaphase nucleolar organizer regions: evidence for a twisted-loop organization. *Mol Biol Cell* **8:** 2199–2216

Jensen CG, Wilson WR, Bleumink AR (1985) Effects of amsacrine and other DNA-intercalating drugs on nuclear and nucleolar structure in cultured V79 Chinese hamster cells and PtK2 rat kangaroo cells. *Cancer Res* **45:** 717–725

Mais C, Wright JE, Prieto JL, Raggett S, McStay B (2005) UBF-binding site arrays form pseudo-NORs and sequester the RNA polymerase I transcription machinery. *Genes Dev* **19:** 50–64

Mayer C, Zhao J, Yuan X, Grummt I (2004) mTOR-dependent activation of the transcription factor TIF-IA links rRNA synthesis to nutrient availability. *Genes Dev* **18:** 423–434

Mayer C, Bierhoff H, Grummt I (2005) The nucleolus as a stress sensor: JNK2 inactivates the transcription factor TIF-IA and down-regulates rRNA synthesis. *Genes Dev* **19:** 933–941

Moss T, Langlois F, Gagnon-Kugler T, Stefanovsky V (2007) A housekeeper with power of attorney: the rRNA genes in ribosome biogenesis. *Cell Mol Life Sci* **64:** 29–49

Németh A, Guibert S, Tiwari VK, Ohlsson R, Längst G (2008) Epigenetic regulation of TTF-I-mediated promoter-terminator interactions of rRNA genes. *EMBO J* **27:** 1255–1265

Olson M (2004) *The Nucleolus*. New York, USA: Kluwer Academic Publishers

Raška I (2003) Oldies but goldies: searching for Christmas trees within the nucleolar architecture. *Trends Cell Biol* **13:** 517–525

Roussel P, André C, Comai L, Hernandez-Verdun D (1996) The rDNA transcription machinery is assembled during mitosis in active NORs and absent in inactive NORs. *J Cell Biol* **133:** 235–246

Russell J, Zomerdijk J (2005) RNA-polymerase-I-directed rDNA transcription, life and works. *Trends Biochem Sci* **30:** 87–96

Wang IC, Chen YJ, Hughes DE, Ackerson T, Major ML, Kalinichenko VV, Costa RH, Raychaudhuri P, Tyner AL, Lau LF (2008) FoxM1 regulates transcription of JNK1 to promote the G1/S transition and tumor cell invasiveness. *J Biol Chem* **283:** 20770–20778

Ye J, Zhao J, Hoffmann-Rohrer U, Grummt I (2008) Nuclear myosin I and polymeric actin act as a molecular motor that drives RNA polymerase I transcription. *Genes Dev* **22:** 322–330

Zhang H, Wang JC, Liu LF (1998) Involvement of DNA topoisomerase I in transcription of human ribosomal RNA genes. *Proc Natl Acad Sci USA* **85:** 1060–1064